12-4-2014

Mitigation of Decubitus Ulcers by Moisture Reduction in Bedridden Catheterized Patients

Kory A. Robinson

MITIGATION OF DECUBITUS ULCERS BY MOISTURE REDUCTION IN BEDRIDDEN CATHETERIZED PATIENTS

by

Kory A. Robinson

A Thesis

Submitted in Partial Fulfillment of the

Requirements for the Degree of

Master of Science

Major: Electrical and Computer Engineering

The University of Memphis

December 2014

ABSTRACT

Robinson, Kory Allan. M.S. The University of Memphis. December 2014. Mitigation of Decubitus Ulcers by Moisture Reduction in Bedridden Catheterized Patients. Major Professor: Dr. Aaron Robinson

In today's society, decubitus ulcers are a serious and very common medical condition. Yet, they constitute a major complication threatening individuals in hospitals, nursing homes and family homecare environments. Decubitus ulcers usually represent a major burden of care and reduces the quality of life considerably for patients, as well as their care givers. Ironically, most patients develop decubitus ulcers after an extended stay in a hospital or acute care facilities. Decubitus ulcers present challenges to the healthcare industry because they are associated with increased risks of bacterial infections, longer hospital stays and higher hospitalization costs. The purpose of this thesis is to develop an approach where moisture accumulation can be effectively reduced by incorporating an automated airflow ventilation system within existing pressure relief mattresses. The proposed design will assist in establishing stability of the patient by regulating the patient's body temperature, as well as, moisture level.

TABLE OF CONTENTS

List of Tables

List of Figures

I. INTRODUCTION

Often, the challenges of managing decubitus ulcers are not limited to clinical decisions only. Decubitus ulcers have a significant impact on the health care system and its wound care providers. Not only that, but decubitus ulcers may also impact other areas that involve patient care including: financial, emotional, psychosocial, regulatory and medical legal aspects. The effort with managing any of these complex factors are magnified by current advances in understanding the pathophysiology of wounds related to pressure, moisture, friction, etc., which serves as the foundation for the etiology, diagnosis, staging and management of these wounds (Niezgoda & Mendez-Eastman, 2006). Understanding the pathophysiology of decubitus ulcers is continuously evolving as research advancement in the area of basic cellular mechanisms and clinical practice continues to rise. It is expected, that enhancing the public's knowledge will improve wound care practitioners' ability to diagnose, treat and more importantly identify at risk patients to prevent decubitus ulcers from its initial development.

A. Originality of Thesis

Within this thesis, a lot of time and effort has been delegated towards developing a new methodology to reduce the accumulation of moisture, by 25%, through an automated airflow ventilation control system with a view to mitigate the development of decubitus ulcers from a patient's body. The goal of this thesis was to lessen the impact of other factors such as friction, shear force and pressure, to name a few, by focusing on the less addressed issue of moisture accumulation.

Since the first implementation of this prototype, careful consideration has been given to ensuring the execution of proper and adequate airflow to provide the most comfort to patients under various temperature and moisture conditions.

B. Previous Research

There are many existing proposed solutions that focus on mitigating decubitus ulcers via pressure reduction. A couple of solutions include: the pressure relief mattress and negative pressure wound therapy. The pressure relief mattress is simply comprised of plastic vibration tubes that inflate and deflate based on a set schedule. On the other hand, the negative pressure wound therapy technique includes a vacuum pump attached to the localized region of the wound, where sub-atmospheric pressure is applied.

One thing that each of the mentioned techniques have in common is that moisture reduction is not of focus, but rather pressure reduction. This is what makes this thesis so unique because the need to address not just pressure only, but the moisture accumulation aspect in combination with pressure reduction is a necessity in increasing the quality of life for all patients. Since there were no developed devices and research geared towards resolving either moisture and pressure issues, or moisture only, the need to develop this prototype as the first of its kind was desirable. With the methodologies implemented within this thesis, the healthcare industry as it is now will change.

C. Decubitus Ulcer Background

Decubitus ulcers are wounds that result from extended periods of continuous pressure on the skin, soft tissue, muscle and bone. Usual at risk patients include the elderly, stroke victims, patients with diabetes, patients with dementia and bedridden patients (any patient with impaired mobility or sensation). These individuals are predisposed to decubitus

ulcers unless they regularly change positions or use other preventive measures, such as pressure reducing mattresses (Russo & Elixhauser, 2006). Figure 1 illustrates the most common areas for decubitus ulcer development (Kroshinsky & Strazzula, 2013).

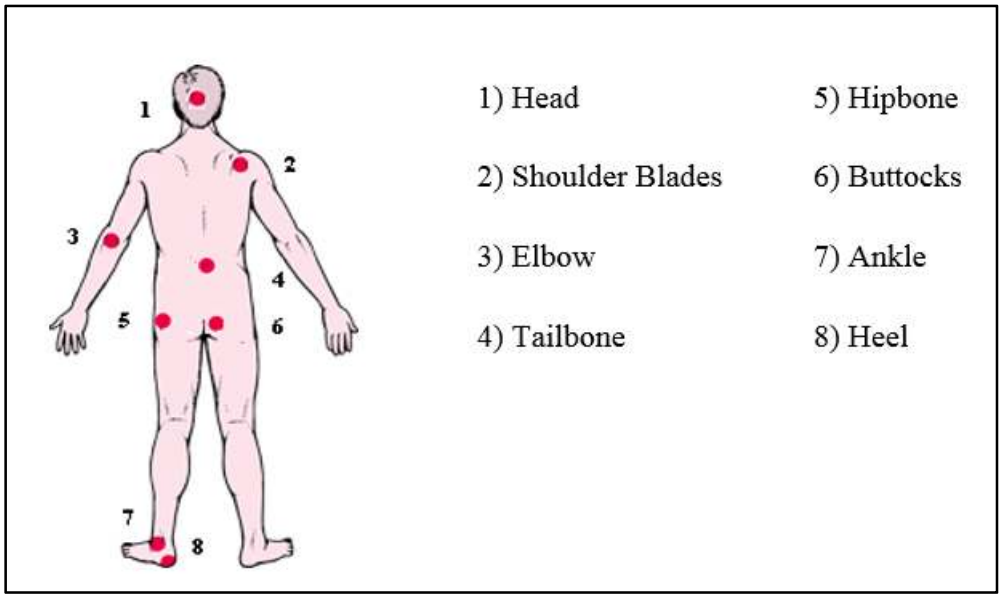

Figure 1. Common areas for Decubitus Ulcer development. From Kroshinsky, D., & Strazzula, L. (2013). *Common Sites for Pressure Sores* [Image]. Retrieved from http://www.merckmanuals.com/home/skin_disorders/pressure_sores/pressure_sore.html?qt=&sc=alt

D. Contributing Factors

Based on the risk for decubitus ulcers, researchers have determined that there is no cut and paste skincare plan that would be beneficial for every patient. Although there are certain components that apply to every skincare plan (cleansing, moisturizing, positioning, nutrition, etc.), the specifications will vary depending on the patient's risk factors and most prevalent circumstances. Nevertheless, circumventing or implementing

steps to counteract known risk factors for decubitus ulcers will help assist in the prevention process (Yuska, 2010). Here are five common contributing factors in the development of decubitus ulcers:

Pressure on the skin, especially over bony regions, acts as a perpendicular force that compresses body tissue and often times result in decreased tissue perfusion and ischemia to that particular region. If the blood flow is restricted for more than 1-2 hours, the region of the skin where pressure is being applied breaks down (Niezgoda & Mendez-Eastman, 2006).

Shear force is typically parallel to the skin's surface. When the head of the bed is raised or a patient slides downward in a chair, the body becomes angulated above the support surface. This causes the skeletal muscle and deep fascia to slide downward with gravity, while the skin and superficial tissues adhere to the chair surface or bed linens. Shear force can cause a change in the angle of the vessels and thus compromise blood supply, resulting in ischemia, cellular death and tissue necrosis (Niezgoda & Mendez-Eastman, 2006).

Friction can often lead to increased progression of decubitus ulcers from one stage to another, by breaking down the outermost layer of the skin (epidermis). Friction of the skin, normally occurs when patients are repeatedly pulled across a surface. Clinically, friction presents as a superficial abrasion of a blister. Shear force and friction often go hand in hand (Perry et al., 2012).

Inadequate Nutrition increases the risk of developing decubitus ulcers and slows down the healing process of developed decubitus ulcers. In the case of malnutrition, patients may not have enough body fat to pad the skin and bones. Eventually, this will

cause severe damage by not having enough body fat to keep the blood vessels from becoming closed. Maintaining a good nutritional diet is important because it provides assistance in the healing process of the body. If the body doesn't get enough calories, protein and other nutrients (especially vitamin C and zinc, which can help heal wounds like decubitus ulcers), the body won't be able to effectively heal, no matter how well one treats the wound ("Bedsores," 2014; Perry et al., 2012).

Moisture can increase skin friction as well as weaken the protective outermost layer of the skin, thus increasing the rate at which the skin breaks down. If the skin is exposed to moisture for extended periods of time, the region may become infected. Sources of moisture accumulation include body perspiration, wound drainage and urine (Thomas, 2001).

E. Decubitus Ulcer Stages

The severity of decubitus ulcers depends upon the amount of damage inflicted onto the skin, soft tissue, muscle and bone regions. Decubitus ulcer damage can range from a change in the color of unbroken skin (Stage I), to severe deep wounds down to the muscle and/or bone region (Stage IV) and often times infects the muscle and/or bone region. As shown below, the severity of decubitus ulcers are characterized into four stages ("Pressure Sores," 2014).

When a Stage I decubitus ulcer begins to develop the localized area of undamaged skin over a bony prominence usually becomes red. The localized area of the undamaged skin may be painful, firm, soft, warmer or even cooler as compared to other adjacent tissue. Darkly pigmented skin may not have any visible blanching and its color may differentiate from the surrounding tissue area, thus making this stage very difficult to

detect in individuals with dark skin tones. (Niezgoda & Mendez-Eastman, 2006; Thomas, 2001). Figure 2 illustrates the initial development on Stage I decubitus ulcers.

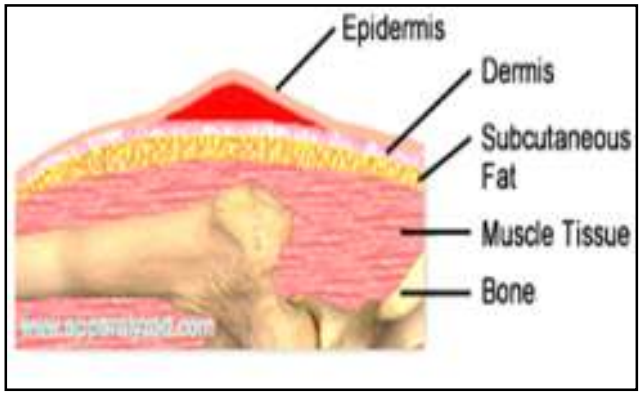

Figure 2. Stage I Decubitus Ulcer. From Pressure Sores, Pressure Ulcers or Decubitus Ulcers. (2014). *Stage I pressure sore* [Image]. Retrieved from http://www.apparelyzed.com/pressuresores.html#stage-one-pressure-sore

As shown in Figure 3, when the Stage I decubitus ulcer transitions into the Stage II category, partial thickness loss of the dermis begins to present a shallow open ulcer with a red/pink wound bed, without fully separating. This could be presented as an intact or ruptured serum-filled blister. During this stage, the appearance can become a shiny or dry shallow ulcer without bruising (Niezgoda & Mendez-Eastman, 2006; Thomas, 2001).

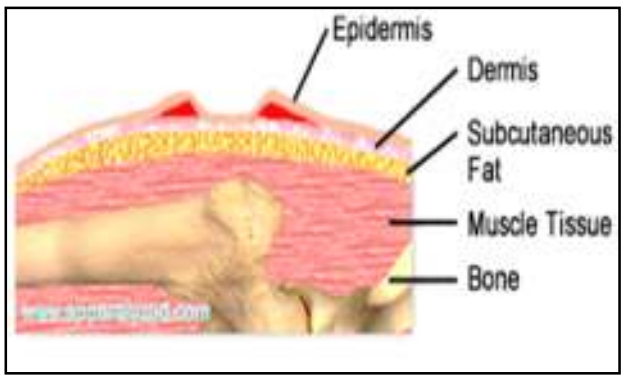

Figure 3. Stage II Decubitus Ulcer. From Pressure Sores, Pressure Ulcers or Decubitus Ulcers. (2014). *Stage II pressure sore* [Image]. Retrieved from http://www.apparelyzed.com/pressuresores.html#stage-two-pressure-sore

Based on Figure 4, during Stage III decubitus ulcer progression, full thickness tissue loss occurs. The subcutaneous fat may be visible, but the bone, tendon or muscles are not exposed. Bruising may be present but does not obscure the depth of tissue loss. The depth of a Stage III decubitus ulcer varies by anatomical location. In contrast, areas of significant accumulation can develop extremely deep craters with or without undermining adjacent tissue (Niezgoda & Mendez-Eastman, 2006; Thomas, 2001).

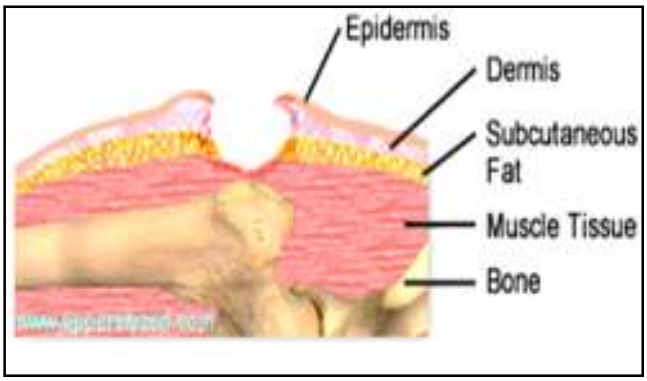

Figure 4. Stage III Decubitus Ulcer. From Pressure Sores, Pressure Ulcers or Decubitus Ulcers. (2014). *Stage III pressure sore* [Image]. Retrieved from http://www.apparelyzed.com/pressuresores.html#stage-three-pressure-sore

When Stage IV develops, as shown in Figure 5, full thickness tissue loss with exposed bone, tendon or muscle occurs. Eschar may be present on some parts of the wound bed. Often times this includes undermining and tunneling tissue area. In addition, the depth of a Stage IV decubitus ulcer varies by anatomical location and often times extend into the muscle and/or supporting structures (e.g., fascia, tendon or joint capsule) making bone infections highly possible (Niezgoda & Mendez-Eastman, 2006; Thomas, 2001).

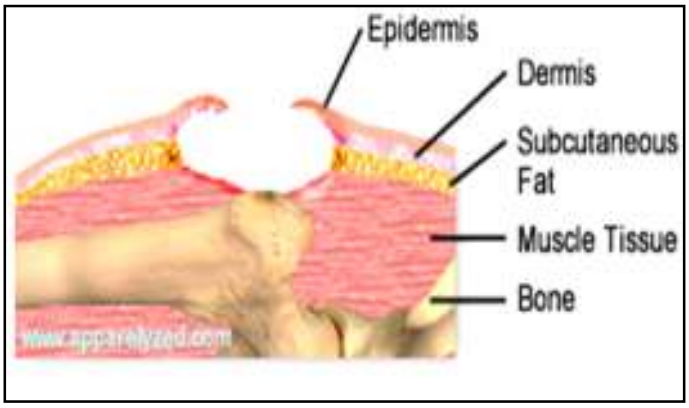

Figure 5. Stage IV Decubitus Ulcer. From Pressure Sores, Pressure Ulcers or Decubitus Ulcers. (2014). *Stage IV pressure sore* [Image]. Retrieved from http://www.apparelyzed.com/pressuresores.html#stage-four-pressure-sore

F. Decubitus Ulcer Impact

According to the National Pressure Ulcer Advisory Panel (NPUAP), incidence is defined as the amount of new cases of decubitus ulcers in a decubitus ulcer free population over a period of time (Dorner, Posthauer & Thomas, 2009). Data from the NPUAP indicates that the incidence of decubitus ulcers varies from 0.4% to 38% in acute care, 2.2% to 23.9% in long term care and 0% to 17% in home care (Niezgoda &

Mendez-Eastman, 2006). Prevalence is defined as a portion of persons who have a decubitus ulcer at any specific point in time (Dorner et al., 2009). Data from the NPUAP also indicates that the prevalence of decubitus ulcers varies from 10% to 18% in acute care, 2.3% to 28% in long term care and 0% to 29% in home care (Niezgoda & Mendez-Eastman, 2006).

With that being said, the impact of decubitus ulcers is very significant as it relates to both monetary and non-monetary costs. In 1999, it was reported that approximately 1.6 million decubitus ulcers develop in acute care facilities in the United States annually, with an estimated yearly cost of $5 to $8.5 billion (Beckrich & Aronovitch, 1999; Niezgoda & Mendez-Eastman, 2006). Now, according to the Joint Commission, more than 2.5 million patients in the United States acute care facilities develop decubitus ulcers, with an estimated yearly cost of 9.2 to 15.6 billion dollars and approximately 60,000 deaths due to decubitus ulcers complications each year (Dorner et al., 2009; Russo, Steiner & Spector, 2008).

The Agency for Healthcare Research and Quality (AHRQ), reported the number of patients developing decubitus ulcers has increased by 63% over the past ten years and that associated hospitalization costs ranged from $16,755 to $20,430 as compared to the average hospital stay of 5 days and costs of approximately $10,000 (Graves, Birrell & Whitby, 2005; Russo, Steiner & Spector, 2008). The Centers for Medicare/Medicaid Services (CMS), reported that the cost of treating a decubitus ulcer in acute care is approximately $43,180 per hospital stay (Dorner, Posthauer & Thomas, 2009). Contributing cost factors include increased length of stay due to decubitus ulcer

complications. Some commonly noted complications were pain, infection progression, support surfaces and decreased functional ability (Dorner et al., 2009).

For instance, in considering infection progression, each Stage III or Stage IV decubitus ulcer can add an additional $14,000 to $23,000 to the overall cost of the patient's care (Beckrich & Aronovitch, 1999). This is primarily due to the fact that more severe decubitus ulcers seldom heal in an acute care facility, which ultimately increases extended care cost. The impact of wound burden in regards to the stage progression, size and amount of the cost of care at long term acute care facilities is very significate. For patients with the highest wound burden, these costs ranged from $50,000 to $70,000 due to longer lengths of stay and higher total daily costs of care, including more nursing care time (Perry et al., 2012; Zhan & Miller, 2003).

G. Perspiration Case Study

The normal perspiration rate to maintain stable body conditions is considered to be $1.5\ \frac{L}{hr}$ or $1500\ \frac{cc}{hr}$ (Nave, 2000). Even though these are considered to be normal maximum levels, water must still be consumed constantly in order to keep the body from dehydrating. After researching, a case study was found that illustrates the effects that increased temperature has on the body's perspiration rate. Two cases were tested where case 1 was executed under normal conditions and case 2 was executed under extreme conditions. For each case, 3 males of excellent physical and mental health were used as test subjects for 2 days. In case 1, the test subjects were covered with rubber sheets and placed on special beds, gently sloped with embedded glass tubes connected to receptacles for perspiration collection (Mosher, 1933).

Perspiration samples at room temperature were collected 3 times daily at 9 am, 3 pm and 11 pm. At each time interval, 200 cc of perspiration was collected from each test subject. Hourly that equates to a perspiration rate of 33.33 $\frac{cc}{hr}$. In case 2, the test subjects were thoroughly cleaned, introduced into a perspiration chamber maintained within 40 ^{o}C to 50 ^{o}C and placed on special beds, gently sloped, with embedded glass tubes connected to receptacles for perspiration collection. After 30-50 minutes of testing, 250 cc of perspiration was acquired, which equates to a perspiration rate of 300 $\frac{cc}{hr}$ (Mosher, 1933). From the data listed above, it was determined that as the temperature increases, whether internally and/or externally, the amount of perspiration that the body produces has the potential to compound exponentially if the body is not sufficiently regulated through adequate airflow ventilation. Given the findings from the perspiration case study, the primary focus of this thesis was not solely to regulate the patient's body temperature and moisture level through airflow ventilation, but to do so in such a way that would be most comfortable and beneficial for the patient. In order to achieve this, effective control of each embedded fan needed to be implemented.

H. Motivation

So why should managing moisture be of focus? According to research, there are certain types of moisture that can cause severe debilitating damage to the skin. Perineal dermatitis, diaper rash, incontinence associated dermatitis or moisture associated skin damage describe some of the conditions caused by moisture from wound drainage, urinary incontinence and perspiration (Zulkowski, 2012). However, regardless of what the condition is called, this damage is very painful and costly. Wounds caused by

moisture are characterized by an erosion of the epidermis and a macerated appearance of the skin (Gray et al., 2007).

Naturally, moisture from any source can increase the skin's permeability and decrease its ability to effectively protect the skin. The outermost layer of the epidermis is marginally acidic and when intact, it prevents the body from acquiring various pathogens. Therefore, if the skin becomes compromised by moisture alone or moisture combined with friction, a break in the surface may occur, thus providing pathogens a medium in which they can enter (Beeckman, Schoonhoven, Verhaeghe, Heyneman & Defloor, 2009; Landefeld et al., 2008). The damaging effects due to friction are escalated when the skin becomes moist. Sliding across bed linens during patient repositioning cause friction to the area of wet skin. Even in patients with containment briefs, the microclimate material between the brief and the skin can become warm and moistened due to perspiration, thus making the skin more susceptible to moisture related damage and friction (Black et al., 2011).

The need to maintain cooler skin temperatures and dryer skin has been discussed on several points between clinicians and researchers. Clinicians and researchers generally recognize the importance of limiting both skin warming and moisture accumulation to effectively prevent skin breakdown. When an area of the skin is warmed beyond approximately 35 ^{o}C (depending on core temperature), local perspiration in the heating region increases noticeably.

As mentioned previously, the accompanying moisture then softens the skin and makes the skin more susceptible to maceration. Not only does moisture due to perspiration provide the skin with instability by weakening the protective outer layers,

but it presents a more severe issue if an area of skin has begun to break. The main issue of concern with decubitus ulcers is keeping the area where the wound has developed clean.

When the consideration of moisture, along with improper wound cleansing comes into account, the probability of the developed decubitus ulcer area becoming infected is considerably increased. If the area becomes infected, this will inevitably decrease the rate at which the infected area will heal and increase the time it takes for the area to fully heal. Signs of an infected pressure sore include the following: thick yellow or green pus, wound becomes odorous, swelling and tenderness, and temperature and pigmentation changes (Zulkowski, 2012).

Treating decubitus ulcers requires a team of healthcare professionals which may include physicians, nurses, dietitians, social workers, pharmacists, occupational and physical therapists. They rely on three principles: pressure relief, care of the wound, and good nutrition to aid in the healing of pressure sores. Most physicians agree decubitus ulcers heal best when they are clean, dead tissue (which may look like a scab) is removed and excessive moisture is kept to a minimum. If not, healing may become decelerated and infection will occur. If a decubitus ulcer is large, deep or does not heal, surgery may be needed to repair any damaged tissue. Even with current medical and surgical therapies, patients who achieve a healed wound have recurrence rates as high as 90%. As the wound heals, it slowly gets smaller. Less fluid drains from it and new healthy tissue starts to grow around the bottom of the wound. This new tissue is typically light red or pink and looks lumpy and shiny. Normally, it may take 2 to 4 weeks of treatment before signs of healing may be seen.

As previously mentioned, the causes of moisture associated skin damage can be very complex. Therefore, managing moisture from perspiration, wound drainage and/or urinary incontinence is an important factor in decubitus ulcer prevention. Since there are currently no devices that addresses both pressure and moisture aspects of decubitus ulcer development with patients, this thesis aims to present a solution to the issue by implementing an approach to assist in increasing stability of the patient by essentially protecting the outermost layers of the skin from prolonged contact with moisture by regulating the patient's body temperature and moisture level with LM35 temperature and Honeywell HIH-4030 RH moisture sensors respectively.

II. METHODOLOGY

The objective of this thesis was to develop an approach where an automated airflow ventilation system could be integrated within existing pressure relief mattresses. By implementing this, the goal would be to effectively minimize the weakening of the outer layers of the skin, due to moisture from body perspiration and/or urine, with bedridden catheterized patients. The design would ultimately provide stability to the skin by reducing the patient's exposure time to moisture, thus helping to protect the outer layers of the skin from prolonged contact with moisture of bedridden patients while decreasing the rate at which decubitus ulcers are developed.

A. Mechanical Prototype

To begin, a simple prototype of a bed with a pressure relief mattress, without the embedded vibration tubes, was designed and assembled. The proposed prototype gives the public an illustration of where and in what manner the automated airflow ventilation system would be integrated into existing pressure relief mattresses. The mechanical prototype consists of the following components: a cushion layer with dimensions of 3' x 2' x 5", an egg crate foam material layer with dimensions of 3' x 2' x 1", a piece of plywood layer with dimensions of 3' x 2' x 1" to be used as the base and 3 Schedule 40 PVC pipes with 3" diameters to be used as airflow ventilation ducts.

Cushion Component: As shown below in Figure 6, 3 holes each with a diameter of 3" were drilled into the side of the cushion in order to embed the Schedule 40 PVC pipes. This is where the Schedule 40 PVC pipes will serve as airflow ventilation ducts.

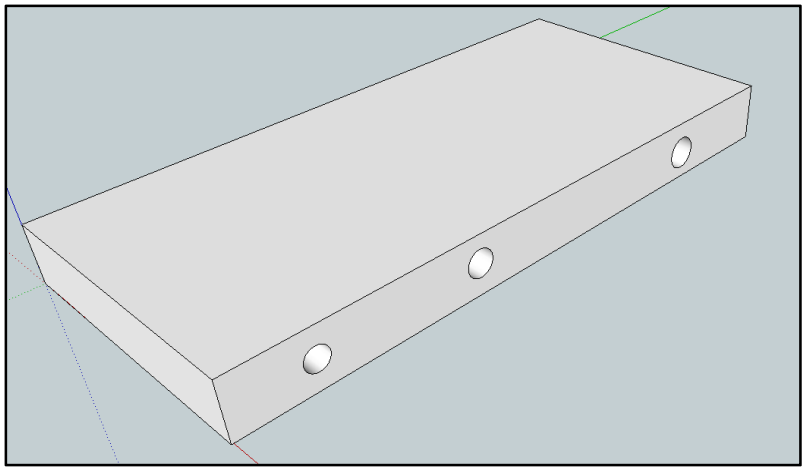

Figure 6. Cushion with embedded 3” Schedule 40 PVC pipes

PVC Pipe Components: Next, several 1” diameter holes were extracted on the top of the 3 holes that contained 3” Schedule 40 PVC pipes, to be aligned with the cushion’s holes, in order to facilitate airflow through the cushion. Figure 7 illustrates the placement of these holes.

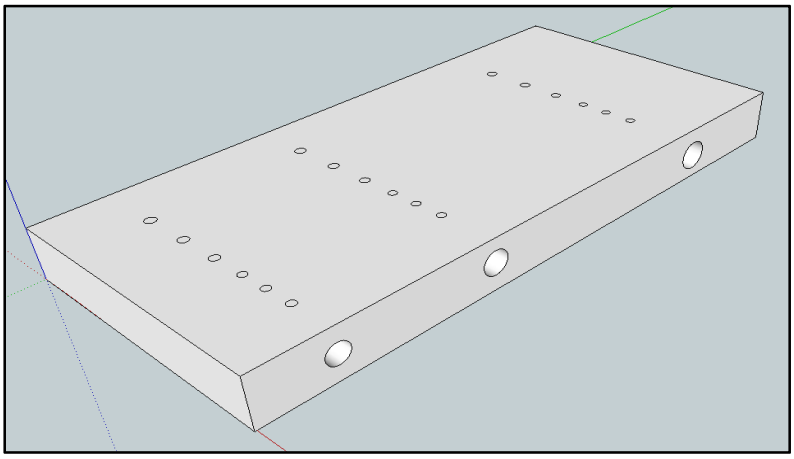

Figure 7. Cushion with 1” diameter airflow ventilation holes

Egg Crate Foam Component: Following the same pattern of the holes as previously shown in Figure 6 and Figure 7, 1” holes were extracted on the egg crate material which will be laid above the cushion where the holes on both layers have the same alignment as shown below in Figure 8. The main purpose of the egg crate foam is to provide elevation and support from the embedded Schedule 40 PVC pipes, so a patient who is laying on the bed prototype will not be able to feel the airflow ventilation ducts.

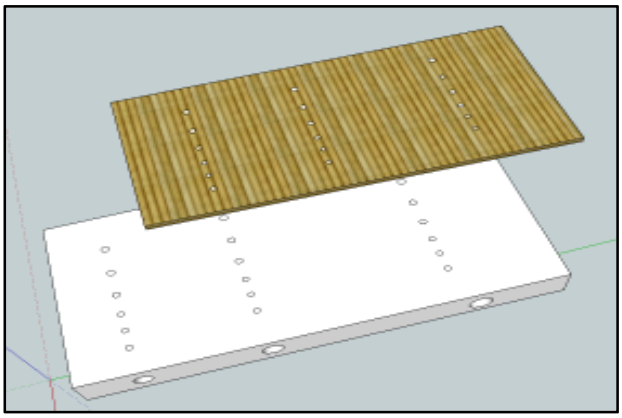

Figure 8. Egg crate foam with 1” diameter airflow ventilation holes

Plywood Component: To provide a solid base under the entire bed, a plywood material was placed at the bottom of the prototype as it is demonstrated below in Figure 9. This provides additional support to the patient to prevent them from sinking into the cushion.

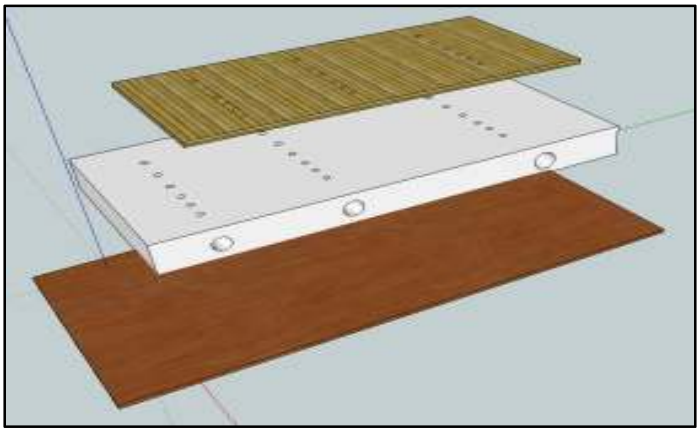

Figure 9. Cushion and egg crate foam with plywood base

B. Electrical / Electronic Prototype

In general, the overall system design is an automated airflow ventilation system. It basically accepts a temperature and moisture input, then produces a mechanical output based the sensor readings. The system design is divided into three levels. As shown in Figure 10, the purpose of the top level, Level 0, is to provide a basic explanation of how the automated airflow ventilation system will function.

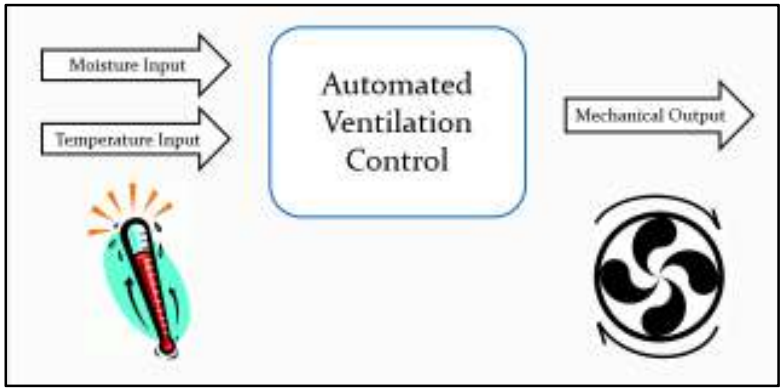

Figure 10. System Design Level 0

The next level of the system design is Level 1. The purpose of this level is to give a brief overview of the system's architecture. Furthermore, this level clearly illustrates the path of signal flow throughout the system. Figure 11 illustrates an overview of the system in detail.

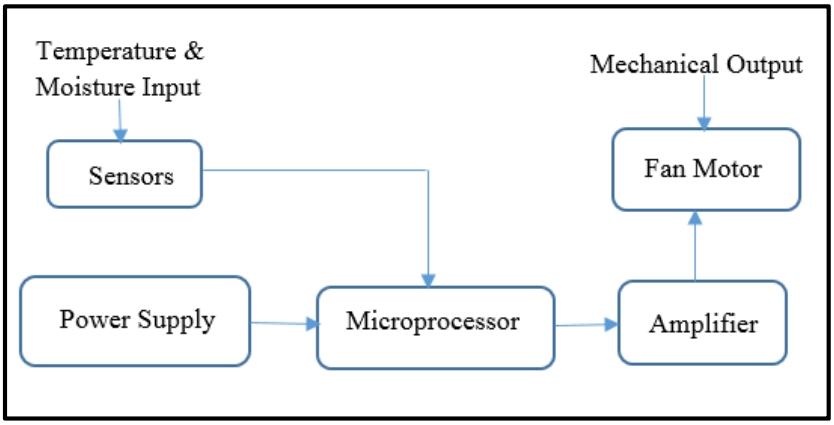

Figure 11. System Design Level 1

The final level encompassing the system design is Level 2. This final level is a more in depth description of the overall electrical design as it includes the actual components that were implemented. The most important of these components are the LM35 temperature sensor, HIH-4030 moisture sensor and the PIC32 microprocessor in regards to the electrical design. These three components are what gives the system design its distinctiveness. Figure 12 illustrates all three levels of the system design.

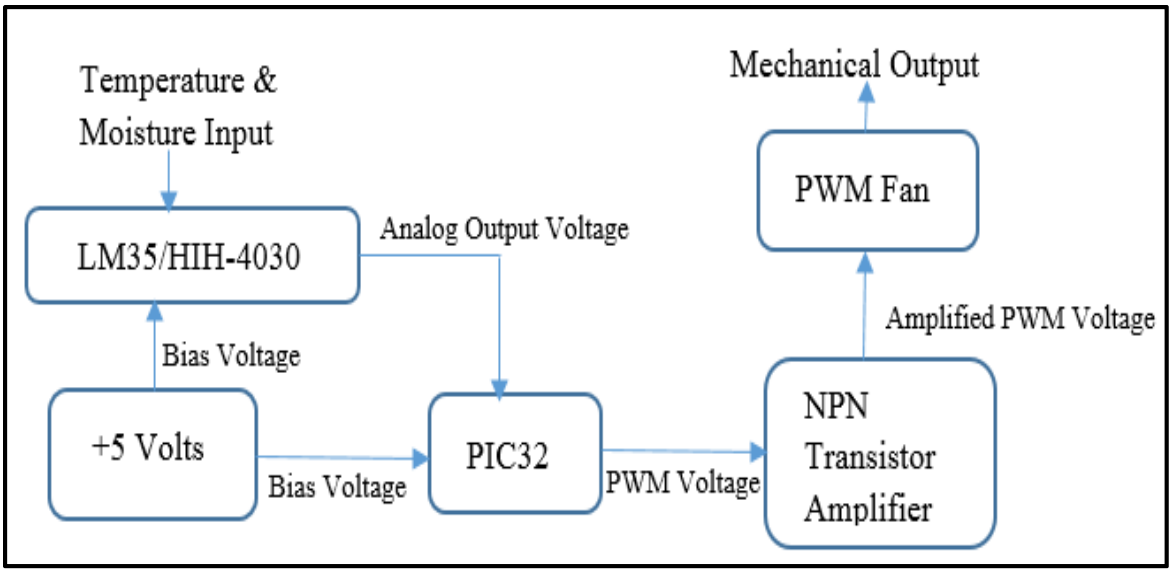

Figure 12. System Design Level 2

C. Functional Decomposition

The electrical control system for the automated airflow ventilation system consists of the following components: PIC32 microcontroller, LM35 temperature sensor package, HIH-4030 moisture sensor package and a NPN transistor current amplifier. The automated airflow ventilation system will sense the temperature level of the patient's critical areas and ambient temperature of the patient's room by embedding LM35 temperature sensors within the egg crate foam material of the prototype and on the control panel. Not only that, but the automated airflow ventilation system will also sense the moisture level of the patient's critical areas by embedding a HIH-4030 moisture sensor in the egg crate foam material of the prototype as well. Calculations will then be performed by the PIC32 microprocessor based on the sensor readings and the NPN transistor will amplify the output signal of the processor such that an appropriate signal to drive each fan motor is attained.

The LM35 temperature sensor, shown in Figure 13, is a transistor type package, which closely resembles an operational amplifier package except that it is much smaller. It has three terminal pins: one for a positive bias voltage in the range of 2.7 to 5 V, a ground pin to connect the device to ground and a center pin that produces an output voltage in the range of zero to the bias voltage, indicating the ambient temperature around the package. Its function is based on the same principle as thermistors, in which the resistance of its components changes with the temperature. The package contains all of the necessary components to perform its operations. The analog output voltage is linearly proportional to the temperature such that a voltage reading of zero is produced at the lowest temperature in its range. According to the chip's data sheets, the range of temperatures that the LM35 will accurately measure ranges from -55 ºC to 150 ºC.

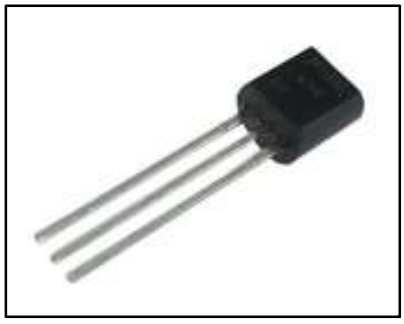

Figure 13. LM35 Temperature Sensor

The HIH-4030 moisture sensor, as shown in Figure 14, is used to measure the moisture percentage level and delivers it as an analog output voltage. The sensor has three terminal pins: one for the positive bias voltage in the range of 4 V - 5.8 V, a ground pin to connect the device to ground and a center pin that produces an output voltage in the range of zero to the bias voltage. This indicates the moisture level around the sensor.

Typically, the sensor will only consume approximately 200 μA. The analog output voltage is linearly proportional to the moisture level, such that a voltage of zero is produced at the lowest moisture accumulation percentage in its range. According to the chip's data sheets, the range of temperatures that the HIH-4030 will accurately operate in, ranges from -40 ºC to 85 ºC.

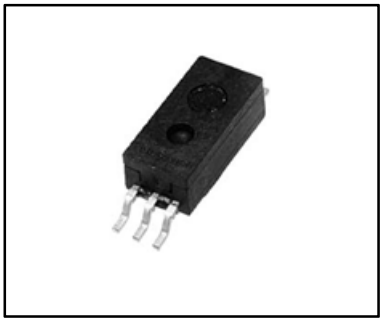

Figure 14. HIH-4030 Moisture Sensor

The output pins of each sensor are connected to the analog input terminal of the PIC32 microprocessor, shown above in Figure 15, and the microprocessor then uses its internal analog to digital converter (ADC) to store the binary value of the each temperature and moisture reading in its memory registers. Certain thresholds, determined through theoretical calculations and experimentation, are programmed in the PIC32 microprocessor using a C/C++ language compiler to activate and deactivate the cooling fans embedded into the prototype. The output signal of the PIC32 microprocessor produces a square wave output signal with a varying duty cycle to deliver more or less power to each fan motor as needed. This square wave output is referred to as a pulse width modulation (PWM) signal due to its ability to vary the amount of power delivered.

For example, if the temperature reading is slightly above room temperature, the high time of the PWM signal will be shorter and if the temperature is well above room temperature, the high time of the signal will be increased to deliver more power to the fans for faster cooling. This same principle was used for the moisture sensor as well.

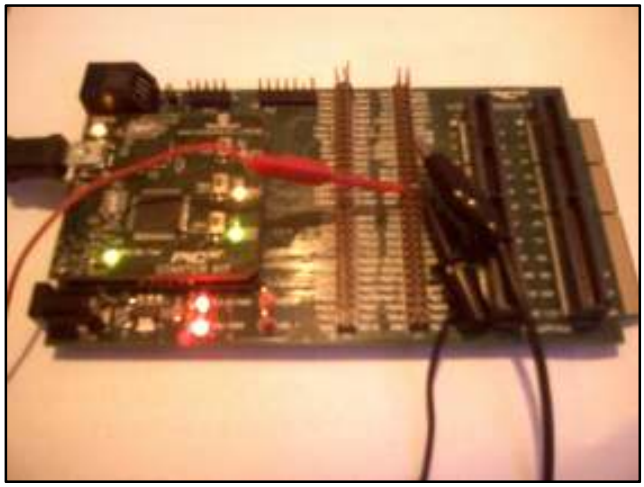

Figure 15. PIC32 Microprocessor

In determining a transistor amplifier that would be suitable in satisfying the operable needs of this prototype, the following criteria needed to be achieved: very high current gain, low voltage gain, high input resistance and low input resistance. The common emitter amplifier has high current and voltage gain, low input resistance and high output resistance. The common base amplifier has very low current gain, high voltage gain, low input resistance and high output resistance. The common collector amplifier has high current gain, very low voltage gain, high input resistance and low output resistance. Considering all of the amplifier configurations, the common collector closely met the design criteria as stated above. The decision to use the Darlington pair, instead of a single

common collector amplifier, was primarily based on the very large current gain it produces (Millman & Grabel, 1987).

As shown in Figure 16, the Darlington pair consists of two bipolar junction transistors connected as common collector amplifiers in such a way that the emitter of one transistor supplies current to the base of the second transistor. With that in mind, the overall current gain of the Darlington pair is equal to the product of the current gain of each common collector. It is also shown in Figure 16, that the PWM output signal from the PIC32 microprocessor drives the Darlington TIP-120 power transistor, such that a suitable current level is delivered through the fan motor coils, which are connected to the amplifier in a common collector configuration.

This transistor consists of two bipolar junction transistors cascaded together in one package with built in base to emitter resistors of 8 $k\Omega$ and 120 Ω, for a dimensionless current gain h_{fe} of 1000. The desired collector current must be strong enough to sufficiently drive each fan motor, while remaining within the current rating of the chosen fans. The square wave PWM signal produces a square wave base current I_B. Therefore, a square wave output current in the collector is produced, which will be amplified by the overall gain of the Darlington TIP-120 power transistor circuit.

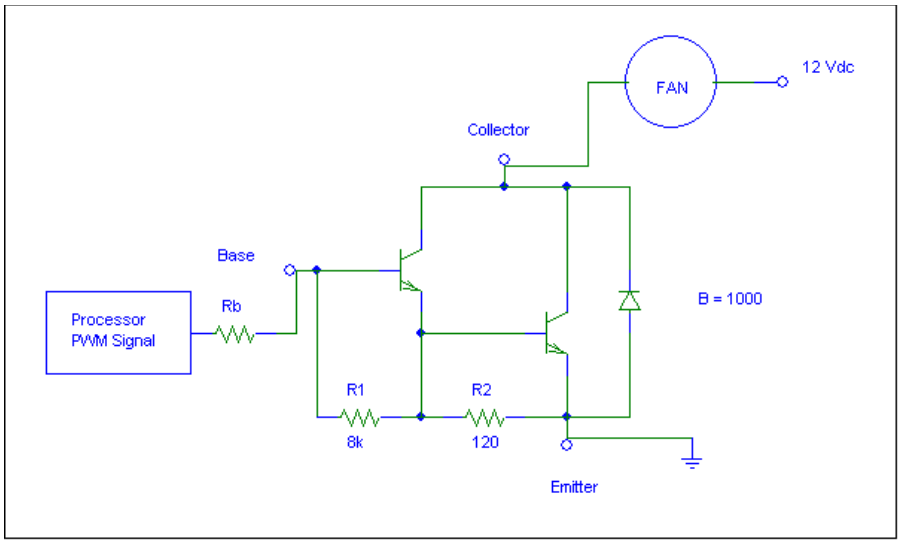

Figure 16. Darlington Pair Schematic

D. Calculations

In order to adequately regulate the fan speed through the Darlington TIP-120 power transistor circuit due to each sensor reading level, appropriate calculations had to first be established. Theoretical values of the output voltage were obtained, using proportionality calculations for each connected sensor. Since the PIC32 microprocessor's ADC is a 10 bit processor and the output voltage of the microprocessor's pins is approximately 3.33 V, each sensor analog signal can be resolved in 2^{10} or 1024 ways. Taking this into consideration, the following proportionality expression was developed as shown in Equation 1.

$$R = \frac{V_{FS}}{2^B} \quad (1)$$

Where R, represented by the resolution of the internal ADC, is equal to the full scale voltage range V_{FS} divided by 2^B. V_{FS}, shown in Equation 2, is the difference between the

high and low reference voltage. For simulation purposes, the high reference voltage is approximately 3.33 V and the low reference voltage is 0 V. B represents the ADC's resolution in bits. In order to capture the true sensor readings, a few conversions had to be implemented.

$$V_{FS} = V_{REFHI} - V_{REFLOW} \tag{2}$$

Airflow Calculations: According to the fan specification sheet, the maximum airflow that each embedded fan can produce is 40.2 CFM at a maximum speed of 3400 RPM. Since the output voltage of the PIC32 microprocessor's pins is approximately 3.33 V, the following proportionality expression was developed, as shown in Equation 3 below, to calculate a corresponding airflow value at 3.33 V.

$$\frac{V_{RATED}}{CFM_{MAX}} = \frac{V_{REFHI}}{CFM_{MAX\_UNKNOWN}} \tag{3}$$

V_{RATED}, which represents the rated voltage of the fan, divided by the maximum airflow CFM_{MAX} is proportional to the high reference voltage of the PIC32 microprocessor divided by an unknown maximum airflow $CFM_{MAX\_UNKNOWN}$. Based on the following, the rated voltage V_{RATED} equaling 12 V, the maximum airflow CFM_{MAX} equaling 40.2 CFM and the high reference voltage V_{REFHI} equaling 3.33 V, $CFM_{MAX\_UNKNOWN}$ was calculated to be 11.16 CFM at 3.33 V. In the Software Implementation section of this thesis, it is noted that the PWM settings for the HIGH, MED and LOW fan levels were based on 100%, 79%, and 0% respectively.

Since the LOW PWM triggers will only occur during normal stable conditions, the focus will be on the HIGH and MED level conditions. After the new maximum airflow of 11.16 CFM or 312.41 $\frac{in^3}{s}$ was captured and set for the HIGH PWM level, the medium airflow was calculated by taking 79% of the new maximum airflow. The airflow for the MED PWM level was calculated and set to 8.82 CFM or 253.73 $\frac{in^3}{s}$. So basically, depending upon the PWM level, the wound area would sense an airflow between 0 and 11.16 CFM. The air velocity for each PWM level was calculated using Equation 4 shown below.

$$v_i = 576 * \frac{q_i}{\pi * {d_i}^2} \quad (4)$$

Where v_i is the air velocity in FPM, q_i is the airflow in CFM and d_i is the duct diameter in inches. Next, the corresponding values for the HIGH and MED CFM levels were inserted in the formula, given that the diameter of the duct is 3", to obtain a velocity for the HIGH and MED CFM levels. v_{HIGH} was calculated to be 227.35 FPM and v_{MED} was calculated to be 179.68 FPM. In regards to air velocity, patient comfort levels are commonly established between 10 to 200 FPM as shown in Table 1 (Bradshaw, 2006). While this is the case, higher FPM values are acceptable for intermittent periods to achieve patient comfort by cooling the skin to reduce moisture accumulation.

Table 1
Subjective Response to Air Motion

Air Velocity (FPM)	Occupant Reaction
0 - 10	Complaint about stagnation.
0 - 50	Generally favorable.
50 - 100	Awareness of air motion. May be comfortable, depending on air motion.
100 - 200	Constant awareness of air motion. Acceptable for short periods.
200 and above	Complaint about being an annoyance.

Table 2 illustrates FPM values as large as 500 FPM (Rosenbaum, 1999). This amount of air speed can be tolerated as long as the patient's temperature and/or moisture level increases to critical ranges. Based on the air velocity calculations for the HIGH and MED PWM levels, it is shown that even at the highest air velocity, the acquired FPM values are within acceptable limits per Table 1 and 2. Research suggests that there's a direct correlation between air velocity and temperature reduction. It is noted that for every 15 FPM increase in air movement above an air velocity of 30 FPM, the body will sense a 1° temperature reduction (Bradshaw, 2006).

Table 2.
Equivalent Comfort Conditions

Temperature °F	RH %	Air Speed (FPM)
76	45	20
76	80	250
72	80	20
80	20	20
80	45	500

The air temperature that each embedded ventilation fan produced was approximately 20 ºC or 68 ºF. With this in mind and by using Equation 5, it was estimated that v_{HIGH} results in a 13° temperature drop and v_{MED} results in a 10° temperature drop.

$$T_{DROP} = \frac{v_{AIR} - 30\ FPM}{15\ FPM} \tag{5}$$

Considering the length of the 3" PVC pipe being 3', the time it takes for the temperature to drop 1 ˚could be solved for. As mentioned previously, for every 15 FPM of air movement above an air velocity of 30 FPM, the body will sense a 1 ˚drop in temperature. By using Equation 6, the time it takes for the temperature to drop 1 ˚was found by dividing the distance that the air travels by its speed.

$$Time = \frac{Distance}{Speed} \tag{6}$$

For example, air traveling 3' at a rate of 45 FPM will take approximately 0.2 minutes or 12 seconds to drop the temperature by 1 ˚. Table 3 shows the corresponding time for HIGH and MED PWM levels. As it relates to airflow, moisture accumulation is attributed to inadequate airflow to a particular region of the body. Inadequate airflow would be considered as air moving very slow or not at all, typically around 0 - 20 FPM. The more air becomes stagnant, the more moisture accumulation and temperature increase the patient will experience.

Table 3.
Airflow Temperature Drop

Air Speed (FPM)	Temperature Drop	Time (minutes)
227	up to 13˚	2.6
179	up to 10˚	2

In order to counteract the effect, the fan speeds were adjusted through PWM in such a way that it would provide airflow up to 20 times more than that of stagnant airflow FPM levels. With this, the time it takes a wound to exude signs of healing would be reduced up to 10%.

LM35 Calculations: Based on the device specification sheet for the LM35, the output reading is expressed in units of $\frac{mV}{℃}$. Once the analog reading of the LM35 sensor is captured by the microprocessor and resolved, that reading is then divided by the scale factor 10.0 $\frac{mV}{℃}$ to obtain a temperature value in ℃.

HIH-4030 Calculations: After the LM35 sensor readings are captured and converted, the HIH-4030 sensor readings are then captured and converted in a similar manner. Based on the device specification sheet for the HIH-4030, the output reading is expressed in units of $\frac{mV}{RH\%}$. Once the analog reading of the HIH-4030 sensor is captured by the microprocessor and resolved, that reading is then converted into a percentage using Equation 7 shown below:

$$RH\% = \frac{READING - ZERO\ OFFSET}{SLOPE} \quad (7)$$

Where RH%, represented by the moisture level, is equal to the difference between the HIH-4030 analog reading and zero offset divided by the slope. According to the device specification sheet, the zero offset is 0.958 V and the slope is 0.0307 $\frac{V}{RH\%}$. The corresponding moisture level percentage was correlated to temperature as shown below in Table 4.

Table 4.
Moisture Correlation Chart

	Relative Humidity (%)										
Room temperature (°F)	**0**	**10**	**20**	**30**	**40**	**50**	**60**	**70**	**80**	**90**	**100**
75	68	69	71	72	74	75	76	76	77	78	79
74	66	68	69	71	72	73	74	75	76	77	78
73	65	67	68	70	71	72	73	74	75	76	77
72	64	65	67	68	70	71	72	73	74	75	76
71	63	64	66	67	68	70	71	72	73	74	75
70	63	64	65	66	67	68	69	70	71	72	73
69	62	63	64	65	66	67	68	69	70	71	72
68	61	62	63	64	65	66	67	68	69	70	71
67	60	61	62	63	64	65	66	67	68	68	69
66	59	60	61	62	63	64	65	66	67	67	68
65	59	60	61	61	62	63	64	65	65	66	67
64	58	59	60	60	61	62	63	64	64	65	66
63	57	58	59	59	60	61	62	62	63	64	64
62	56	57	58	58	59	60	61	61	62	63	63
61	56	57	57	58	59	59	60	60	61	61	62
60	55	56	56	57	58	58	59	59	60	60	61

After the associated conversion values for each sensor have been acquired, the PWM of the PIC32 microprocessor will adjust its output voltage driving the Darlington TIP-120 power transistor according to each sensor reading. Given that both the input and output of the Darlington TIP-120 power transistor will be DC signals, basic DC bias calculations were used to determine the value of the base resistance R_b such that the desired collector

current would be reached. Equations 8 and 9, as shown below were used determining the value of the base resistance R_b and the base current I_B.

$$R_b = \frac{V_B}{I_B} \tag{8}$$

$$I_B = \frac{I_C}{h_{fe}} \tag{9}$$

Referencing Figure 16, it is shown that each fan is operated by a Darlington TIP-120 power transistor. The chosen fans maximum ratings are 12 V at 340 mA. In order to run the fans at their rated current level, a base current I_B of 340 μA was needed such that the collector current I_C would draw the maximum rated 340 mA. This was achieved by the dividing I_C, which is equal to the maximum current rating of the fans, by a dimensionless current gain of 1000. With this in mind, R_b was calculated using Equation 8. Where V_B, the base voltage, is equal to 3.33 V and I_B is equal to 340 μA. Therefore the value of R_b was determined to be 9.80 $k\Omega$.

Each fan was wired in series with the collector and biased with a 12 V power supply. Since there are 4 fans and each would draw 340 mA for a total of 1.36 A, a suitable source with a 5 A rating was chosen. Based on this information, the total power consumption was calculated using Equations 10 through 13:

$$P_{Consumption} = I \times V \times N \tag{10}$$

$$P_{Consumption} = I^2 \times R \times N \tag{11}$$

Where I represents current, V represents voltage, R represents resistance and N represents the number of fan components. The total power consumed by the ventilation and cooling fans was:

$$P_{Fans} = 340\ mA \times 12\ V \times 4 = 16.32\ W \quad (12)$$

The total power consumed by the transistor base resistors was:

$$P_{Base} = 340\ \mu A^2 \times 9.80\ k\Omega \times 3 = 3.39\ mW \quad (13)$$

Since the PIC32 microprocessor is powered by a laptop via USB, the overall power consumption is approximately 16.32 W.

E. Software Implementation

For the software implementation phase, (3) LM35 temperature sensors, 2 for patient monitoring and 1 for room monitoring, (1) HIH-4030 RH moisture sensor and (1) tone generator were interfaced with the PIC32 microprocessor to communicate with a PC by way of USB. Essentially, the PC is communicating with the PIC32 and the PIC32 is then communicating with each connected analog sensor device to capture the corresponding sensor reading as shown below in Figure 17.

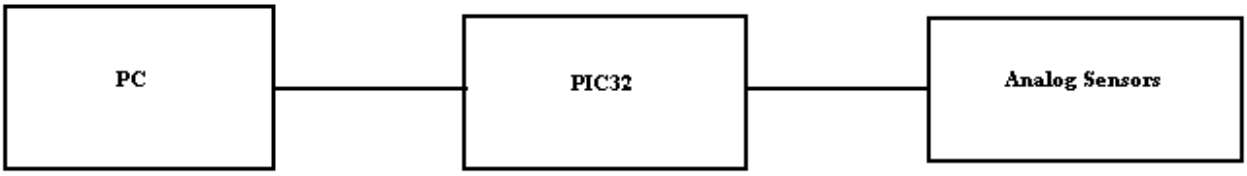

Figure 17. Communication Block Diagram

As previously mentioned, when the program is executed, the analog voltage values are read from each sensor by the ADC pins of the PIC32 microprocessor and resolved to a representative value. With obtaining the calculated resolved values, proportionality calculations were derived according to the device specification sheet for each sensor to extract the corresponding temperature in ^{o}C for the LM35 and the corresponding moisture percentage for the HIH-4030.

After resolving and converting the sensor signals into their respective values, conditionals to set the microprocessor's PWM to control the actual fan speed, based upon temperature and moisture levels, had to be decided. Table 5 shows the event conditionals that were used in determining suitable levels that would increase patient comfort, all while controlling their temperature and moisture level. Once any of the following conditions have been detected, the fan speed and sound alert will respond appropriately.

Table 5.
Program Event Conditionals

Sensor Reading	Program Conditions	Fan Speed	Alert
Patient Temperature	Temp _P > 102˚F	HIGH	YES
	98.9˚F < Temp_P ≤ 102˚F	HIGH	NO
	96.0˚F < Temp_P ≤ 98.9˚F	MED	NO
	Temp_P ≤ 96.0˚F	LOW	NO
Ambient Temperature	Temp_R > 79.9˚F	HIGH	NO
	74.0˚F < Temp_R ≤ 79.9˚F	MED	NO
	Temp_R ≤ 74.0˚F	LOW	NO
Moisture	RH_Level > 70%	MED	YES

Based on the datasheet for the PIC32 microprocessor, the PWM was setup with an optimal system frequency of 80 MHz. Since the PIC32 microprocessor ADC is connected to the peripheral bus, the frequency of the peripheral bus (FPB) had to be set. For practical purposes, it was decided to utilize a frequency of 36 MHz due to its commonality in similar applications. Next, the sample rate of the PWM frequency had to be defined and 5 kHz was chosen. Considering the inverse relationship between the period and frequency, the sampling rate interval time was calculated to be 200 μs. This would equate to approximately 1440 instructions to be executed at a minimum system frequency of 72 MHz. With these program declarations established, a maximum PWM equation was derived as shown below in Equation 14.

$$PWM_{MAX} = \frac{FPB}{SAMPLING\ RATE} \tag{14}$$

As stated previously, the FPB is 36 MHz and the sampling rate is 5 kHz, therefore the max PWM was calculated to be 7200 steps. This means the timer interrupt will occur

every 7200 steps from 0% to 100% modulation. After the system frequency, sampling rate, FPB and max PWM were defined, the fan speed levels: HIGH, MED and LOW, were set based on the PWM settings at 100%, 79% and 0%. The PWM settings for the MED fan speed level was chosen based on trial and error due to the fan speed operating at the same level as the LOW speed PWM setting for a PWM of 50%.

III. RESULTS

A. Fabrication

The prototype was successfully constructed using the aforementioned materials noted in the Mechanical and Electrical/Electronic Prototype sections of this paper. The body of the prototype was assembled with a finished plywood base, alternating rows of foam padding for support and 3” Schedule 40 PVC pipes as shown in Figure 18.

Figure 18. Cushion with embedded 3” Schedule 40 PVC pipes

Next, an egg crate foam layer consisting of 1” diameter holes was attached to the top of the foam padding to protect the patient. One inch diameter holes were extracted from the medical egg crate foam and aligned with 1” diameter holes drilled into 3” Schedule 40 PVC pipes, in order to provide air flow ventilation. The 3” Schedule 40 PVC pipes were capped on one end and fans were affixed to the other end, as shown in Figure 19 and Figure 20, such that air would enter through the fan body, pass through the 3” Schedule 40 PVC pipes and vent through the top layer of the foam. This provides airflow

ventilation to reduce the moisture accumulation and temperature level of the pressure relief mattress, as well as the patient's skin.

Figure 19. Cushion with 1" diameter airflow ventilation holes (Left Side)

Figure 20. Cushion with 1" diameter airflow ventilation holes (Right Side)

The electrical control panel was assembled separately from the mattress prototype for the purpose of isolating sensitive electronic components such as the power supply and the PIC32 microprocessor. With doing so, this placed the prototype design within

National Electric Code (NEC) standard 517.80 for medical devices by separating it from the control system (Earley, Coache, Cloutier & Moniz, 2013). Figure 21 and Figure 22 illustrates the control panel separate from the actual prototype.

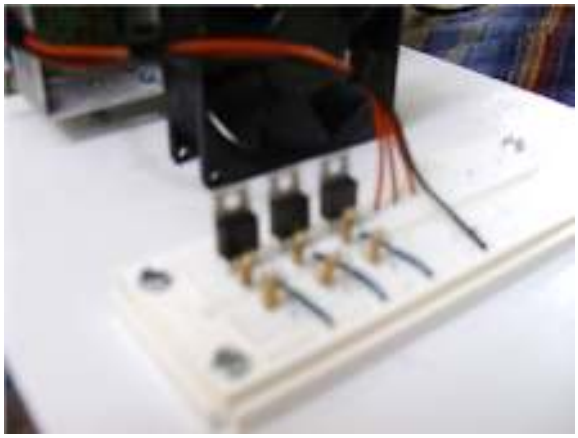

Figure 21. Darlington transistor circuit on control panel

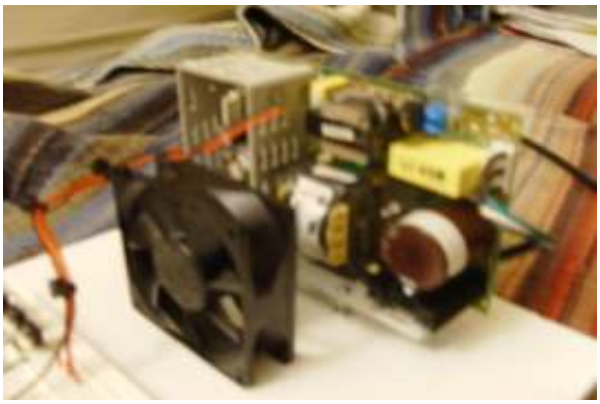

Figure 22. Power supply on control panel

Other materials used included: insulating heat shrinks for solder joints, electrical tie wraps and plastic flexible conduit for covering all conductor wiring between the mattress and control panel. This protects the patient from accidental contact with any conductor and deter wires from becoming damaged. As shown in Figure 23 and Figure 24, these materials were used to satisfy the requirements for NEC standard 517.82 (Earley et al., 2013).

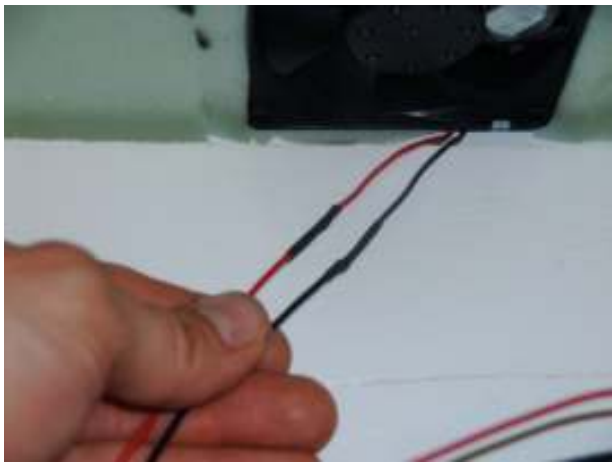

Figure 23. Insulating Heat Shrink

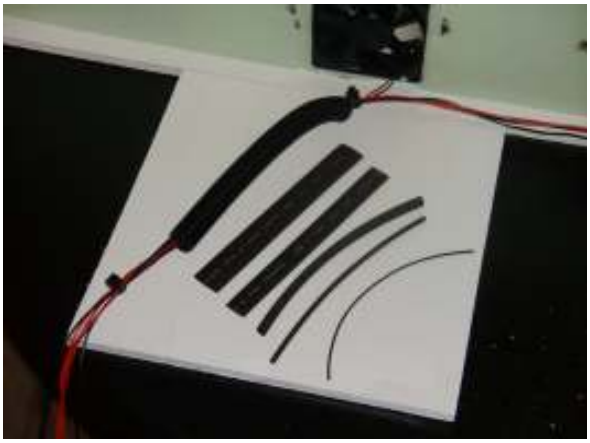

Figure 24. Flexible Conduit and Electrical Tie Wraps

B. Airflow Testing

Producing proper and adequate airflow has been the point of interest in reducing moisture accumulation because it directly impacts the patient in regards to healing and comfort. The initial thought behind developing an automated airflow ventilation system was to have one constant airflow level regardless of the patient's current moisture and temperature condition. The issue is that patient comfort was not incorporated, versatility and control was limited and the potential to create more medical issues was increased.

The first test, Test 1, was used to set a starting point. The test used a 5 V source that was applied to the input terminal of the Darlington pair transistor in order to drive the ventilation fans. It was noted, that Test 1 produced an airflow of 16.75 CFM or approximately 341 FPM for all patient moisture and temperature levels. Another test, Test 2, was performed with 3.33 V being the input voltage, supplied by the PIC32, and stepped down proportionally for the HIGH, MED and LOW PWM levels.

It was also noted, that for HIGH PWM, 3.33 V produced an airflow of 11.16 CFM or approximately 227 FPM and for MED PWM, 2.63 V produced an airflow of 8.82 CFM or approximately 179 FPM. Based on the subjective response to air motion, it is shown that Test 2 provided the best results in terms of providing adequate airflow and maintaining acceptable patient comfort levels. Therefore, Test 1 was rejected and Test 2 was accepted and implemented.

C. Software Simulation

The goal of the software simulation phase was to utilize derived mathematical models as a way to reproduce the actual characteristics of a designed electrical circuit. To recall from the Software Implementation section, when the program is compiled and executed,

analog voltage values are read from each connected sensor by the ADC pins of the PIC32 microprocessor and then resolved to a corresponding digital value. With the calculated resolved values, proportionality calculations according to the data sheet parameters of each sensor were derived to extract a temperature reading in ^{o}C for the LM35 and a correlating moisture percentage for the HIH-4030.

After extracting a representative value for each sensor signal, conditionals to set the PWM to control the fan speed based upon various temperature and moisture levels were incorporated according to the subjective response to air motion. From that, suitable levels that would increase patient comfort, all while controlling their temperature and moisture level were developed. For testing purposes, a hair dryer was used as a variable heat generator in order to trigger each event condition defined. Figure 25 is the response of the PIC32 microprocessor and Figure 26 is a screenshot of the actual code being executed under normal conditions. The status light on the PIC32 is yellow, based on this case, which indicates normal operating conditions.

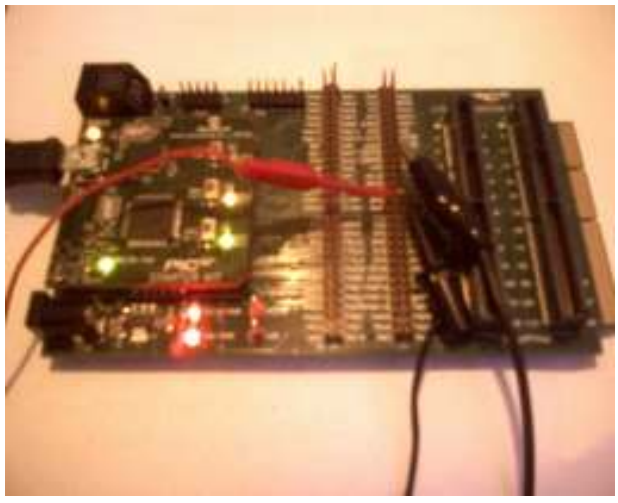

Figure 25. PIC32 Normal Conditions

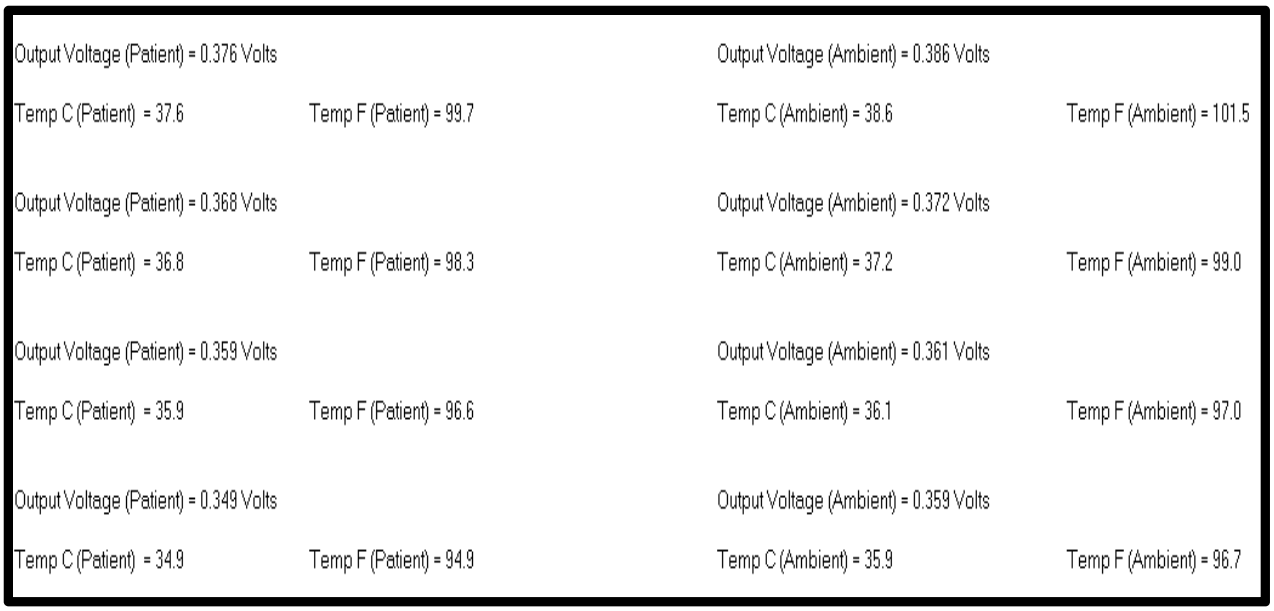

Figure 26. Software Simulation Normal Conditions

In order to test the full functionality of the prototype, the software was executed under abnormal conditions. The abnormal condition in this case was an excessively high moisture accumulation level, which was simulated by using a cup of hot steamy water to replicate body perspiration. Figure 27 is the response of the PIC32 microprocessor, but in comparison to the PIC32's response in Figure 25, the status light switched from yellow to red indicating that critical levels have been reached. It is shown in Figure 28, when conditions reach a defined critical level, an alert is sounded and then displayed to the primary caregiver until the issue has been completely rectified.

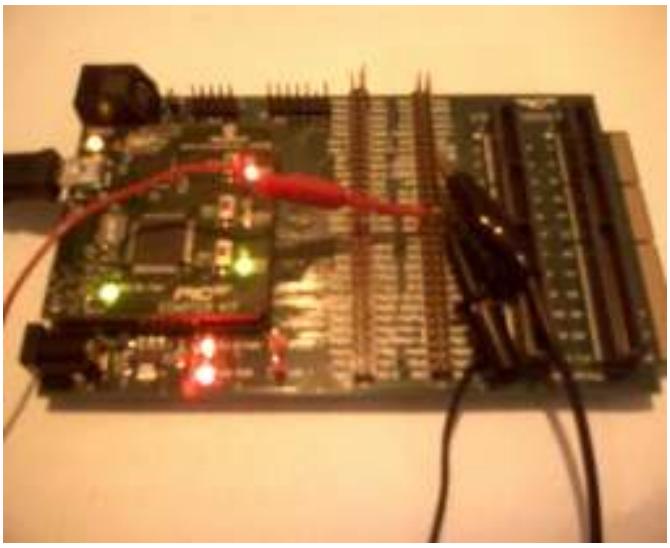

Figure 27. PIC32 Critical Conditions

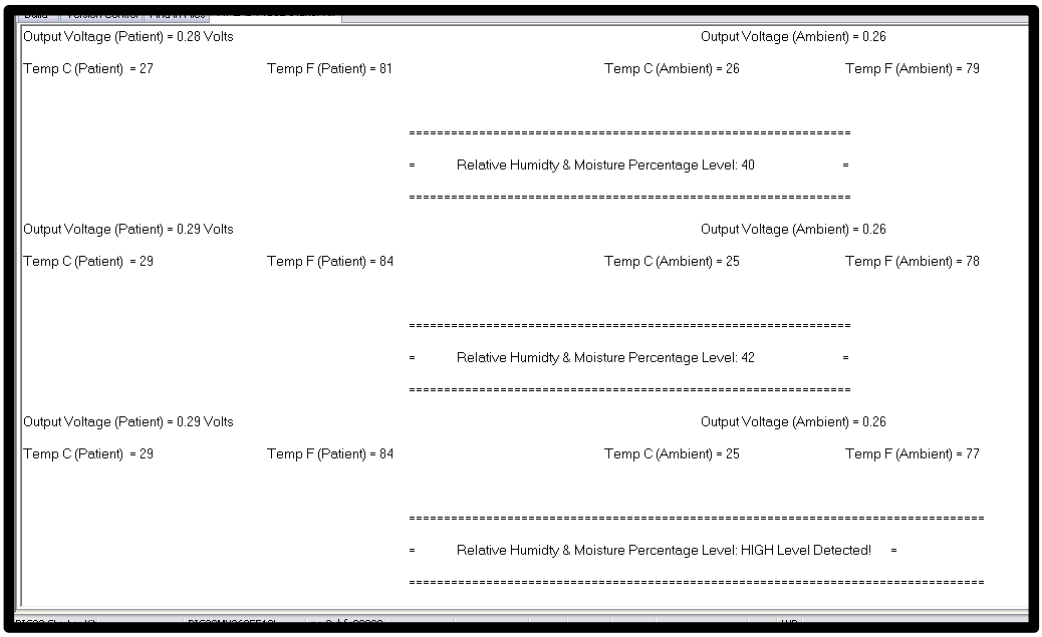

Figure 28. Software Simulation Critical Conditions

IV. DISCUSSION AND CONCLUSION

A. Discussion on Findings

When researching various treatment regiments for preventing or managing decubitus ulcers, it's amazing to see numerous devices used to solve issues dealing with pressure, but limited solutions for reducing moisture accumulation. Contrary to popular belief, moisture has and still is continuously presenting problems within the health care industry (Dorner et al., 2009). It has been shown, that moisture working in combination with pressure and friction can be very problematic by increasing the development rate and overall healing time of decubitus ulcers (Dorner et al., 2009).

As a result, each year, billions of dollars are allocated to the efforts of wound care. This sheds light on the very large number of patients requiring wound care treatment. The purpose of this thesis was to simply develop an approach where the weakening of the outermost layers of the skin, due to moisture from body perspiration and/or urine with bedridden catheterized patients, could effectively be minimized by incorporating an automated airflow ventilation system within existing pressure relief mattresses. Although the proposed design won't entirely prevent the development of decubitus ulcers, it is believed that addressing the issue of moisture accumulation in conjunction with other preventative/management tools, could reduce the hospitalization time, treatment costs, healing time up to 10% and increase the overall quality of life for each patient.

B. Conclusion

Decubitus ulcer prevention is key to ensuring the physical and psychological well-being of patients. Managing moisture from body perspiration, incontinence and possible wound drainage are important factors in the prevention process. Moisture accumulation

due to body perspiration, incontinence and wound drainage are prevalent in millions of people world-wide. Yet, this issue has been inadequately discussed and not routinely assessed as part of general patient medical care. This is very problematic for aging adults whose skin changes create a higher probability for moisture associated skin damage.

In order to address these issues, two tests were implemented to see which one would yield the best healing time reduction results, all while maintaining the highest level of patient comfort. It was determined that Test 1 produced the highest airflow, approximately 1.5 times more than the HIGH PWM level for Test 2, but patient comfort was sacrificed. The level of airflow for Test 1 was considered as an annoyance for extended periods of time, based on Table 1.

On the other hand, Test 2 deemed to provide the best results in regards to maintaining adequate airflow at HIGH, MED and LOW PWM levels, as well as provide appropriate levels of comfort for the patient. Even though the airflow at the HIGH PWM level was slightly higher than the patient comfort threshold, the result is still acceptable, given the airflow will only remain at this level for short intermittent time periods in the healing/mitigation process. Therefore, Test 1 was rejected and Test 2 was implemented. It was shown, that the healing time did not yield a 25% reduction, but rather 10%.

Consideration should be given to the fact that simulations and associated calculations were taken from the moisture and temperature reduction perspective. With this in mind, it is estimated that the overall healing time could potentially exceed a 25% reduction once pressure relief is taken into account. Of course, further testing will need to be implemented for verification purposes.

C. Recommendations for Future Research

While this thesis has achieved its primary objective of implementing an airflow ventilation system as a means to reduce the accumulation of moisture, there are still a few things that are on the agenda for further research and implementation. One major change is to develop a three tier zoning system, where each area of the mattress that has an embedded air duct and ventilation fan can operate independently of each other. For example, if the upper back region needs to be cooled and it is located in zone 1, the other zones will not trigger airflow if it is not warranted. Within each of those zones, the air ducts that were once Schedule 40 PVC pipe, will be replaced with flexible PE tubing considering PVC being more brittle than PE. This will provide more comfort for the patient and increase the integrity of the airflow ventilation system. Next, a more extensive analysis of airflow as it relates to healing at each stage level of decubitus ulcers and the actual reduction percentage for each stage should be addressed. Lastly, deploying and testing the prototype on actual patients in nursing homes or hospitals is of interest as well.

REFERENCES

Beckrich, K., & Aronovitch, S. A. (1999). Hospital acquired pressure ulcers: A comparison of costs in medical vs surgical patients. *Nursing Economics, 17*(5), 263-271.

Bedsores. (2014, March 25). Retrieved from http://www.mayoclinic.org/diseases-conditions/bedsores/basics/definition/con-20030848

Beeckman, D., Schoonhoven, L., Verhaeghe, S., Heyneman, A., & Defloor, T. (2009). Prevention and treatment of incontinence-associated dermatitis: Literature review. *Journal of Advanced Nursing, 65*(6), 1141-1154.

Black, J. M., Gray, M., Bliss, D. Z., Kennedy-Evans, K. L., Logan, S., Baharestani, M. M., Colwell, J. C., Goldberg, M & Ratliff C. R. (2011). MASD part 2: Incontinence-associated dermatitis and intertriginous dermatitis: A consensus. *Journal of Wound, Ostomy and Continence Nursing, 38*(4), 359-370.

Bradshaw, V. (2006). *The Building Environment: Active and Passive Control Systems* (3rd ed., pp. 20-21). New Jersey: Wiley.

Dorner, B., Posthauer, M., & Thomas, D. (2009). The role of nutrition in pressure ulcer prevention and treatment: National pressure ulcer advisory panel white paper. *Advances in Skin & Wound Care, 22*(5), 212-221.

Earley, M. W., Coache, C. D., Cloutier, M., & Moniz, G. (2013). *National Electric Code 2104*. (13th ed., p. 482). Quincy, MA: National Fire Protection Association.

Graves, N., Birrell, F., & Whitby, M. (2005). Effect of pressure ulcers on Length of Hospital Stay. *Infection Control and Hospital Epidemiology, 26*(3), 293-297.

Gray, M., Bliss, D. Z., Doughty, D. B., Ermer-Seltun, J., Kennedy-Evans, K. L., & Palmer, M. H. (2007). Incontinence-associated dermatitis: A consensus. *Journal of Wound, Ostomy, and Continence Nursing, 34*(1)*,* 45-54.

Kroshinsky, D., & Strazzula, L. (2013). *Common Sites for Pressure Sores* [Image]. Retrieved from http://www.merckmanuals.com/home/skin_disorders/pressure_sores/pressure_sores.html?qt=&sc=&alt

Landefeld, C.S., Bowers, B.J., Feld, A.D., Hartmann, K.E., Hoffman, E., Ingber, M.J., et al. (2008). National Institutes of Health State-of-the-Science Conference Statement: Prevention of fecal and urinary incontinence in adults. *Annals of Internal Medicine*, *148*(6), 449-458.

Millman, J. & Grabel, A. (1987). *Microelectronics* (2nd ed., pp. 420). New York: McGraw-Hill.

Mosher, H. H. (1933). Simultaneous study of constituents of urine and perspiration. *The Journal of Biological Chemistry*, *99*(3), 781-790.

Nave, R. C. (2000, July 02). *Perspiration cooling of body*. Retrieved from http://hyperphysics.phy-astr.gsu.edu/hbase/thermo/sweat.html#c1

Niezgoda, J. A., & Mendez-Eastman, S. (2006). The effective management of pressure ulcers. *Advances in Skin & Wound Care, 19*(1), 3-15.

Perry, D., Borchert, K., Burke. S., Chick, K., Johnson, K., Kraft, W., Patel, B., & Thompson, S. (2012). Institute for clinical systems improvement. *Pressure Ulcer Prevention and Treatment Protocol*.

Pressure Sores, Pressure Ulcers or Decubitus Ulcers. (2014). [Image]. Retrieved from http://www.apparelyzed.com/pressuresores.html

Rosenbaum, M. (1999, October 07). *Passive and low energy cooling summary*. Retrieved from http://www.buildinggreen.com/features/mr/cooling.cfm#1.0

Russo, C. A., & Elixhauser, A. (2006). Hospitalizations Related to Pressure Sores, 2003. *HCUP Statistical Brief*.

Russo, C. A., Steiner, C., & Spector, W. (2008). Hospitalizations related to pressure ulcers, 2006. *HCUP Statistical Brief*.

Thomas, D. R. (2001). Prevention and treatment of pressure ulcers: What works? What doesn't? *Cleveland Clinic Journal of Medicine, 68*(8), 704-722.

Yuska, C. (2010). *Understanding Risk Factors in Pressure Ulcer Development and Wound Healing*. Retrieved from http://www.medline.com/media/assets/pdf/Understanding-Risk-Factors-in-Pressure-Ulcer-Development-and-Wound-Healing.pdf

Zhan, C., & Miller, M. R. (2003). Excess length of stay, charges, and mortality attributable to medical injuries during hospitalization. *JAMA: The Journal of the American Medical Association, 290*(14), 1868-1874.

Zulkowski, K. (2012). Diagnosing and treating moisture-associated skin damage. *Advances in Skin & Wound Care, 25*(5), 231-236.